# Numerical study of irreversible aggregation process in three dimensional polymer and surfactant systems

Tomàs Sintes
*Departament de Física, Universitat de les Illes Balears, E-07071 Palma de Mallorca, Spain*
Raúl Toral
*Departament de Física, Universitat de les Illes Balears, E-07071 Palma de Mallorca, Spain*
Amitahba Chakrabarti
*Physics Department, Kansas State University, Manhattan, Kansas 66506*

(Received 8 August 1990; accepted 26 December 1990)

We present the results of numerical simulations of the irreversible aggregation process for self-avoiding flexible polymers in three dimensions. We have paid special attention to two experimentally interesting systems: telechelic ionomers and reverse micelles. The dynamics used in this paper to simulate the clustering process is based on Eden's method. This dynamics was previously introduced by us for two-dimensional systems. We find a scaling relation between the radius of gyration of the cluster $R_g$, the chain length $n$ and the number of chains $N$ in the cluster in the form $R_g \sim n^{\alpha} N^{\beta}$. The values of the exponents $\alpha$ and $\beta$ calculated from the numerical simulations are somewhat lower than those predicted by Flory's classical theory. We argue that the lower values of the exponents are possibly due to the finite size of the clusters and the presence of higher order interaction terms not considered in Flory's theory.

## I. INTRODUCTION

In recent years there has been an increasing interest in the subject of aggregation of self-associating polymer systems.[1] These systems are formed by long flexible macromolecules that contain one or more associating sites which strongly attract each other and lead the chain molecules to aggregate and form clusters. The characteristic geometry of these aggregates is responsible for their unusual physical properties which, in turn, account for their technological importance. Examples of this aggregation process are the aggregation of ionic polymers[2-6] (or ionomers, as they are known in the literature) and the formation of micelles[7-9] and reverse micelles.[8,10,11]

The telechelic ionomers[12] are a particular case of ionomers which contain just two ionic functional groups located one at each end of the chain. These functional or "active" groups interact via short-range forces which mediate the formation of structures which are relevant in several self-assembling processes, like the mesophase formation in liquid crystals with disklike molecules,[13] block copolymers and gel formation,[14] as well as the formation of microemulsions.[8]

Formation of micelles and reverse micelles is also of increasing theoretical interest[7-10] as an example of a self-associating system. Although there are many studies about the details of micelle formation, relatively little is known about reverse micelles. These are colloidal structures formed by surfactant molecules in nonpolar solvents. The polar head groups of the surfactant molecules comprise the core of the aggregate and the hydrofobic tail face the nonpolar solvent. Reverse micelles are of practical interest[11] because of their viability as solubilizing agents, catalysts, etc. Their ability to take up water in the polar core allows these structures to be useful for production of paints and lubricants and for effective delivery of drugs. Also, simplified models of reverse micelles have become useful to imitate biological structures such as the cellular membrane.

Despite the experimental evidences about self-association on the systems described above, it seems to be a very difficult task to explain the details of the clustering process as well as the size, shape, and stability of the aggregates. At this stage it seems that computer simulations of simple models, which allow to control and isolate the essential parameters that play an important role and influence the morphology of the aggregate, would help us in the understanding of the macroscopic properties of these structures. The models could then help to identify the relevant features that contribute to the aggregation process.

Following this direction, numerical simulations have been carried out recently. These works have studied the clustering process in two and three-dimensional lattice systems on which polymer chains are modeled by self-avoiding random walks. The first studies were those of Balazs and coworkers[15-17] who extended the well known diffusion limited aggregation (DLA)[18] model, previously used in single particle aggregation, to the clustering process of long chains molecules with one or more associating sites ("sticker sites"). In their model one new chain at a time is released at a far distance from a seed chain and executes a random walk until, eventually, one of its stickers finds another sticker site belonging to the growing aggregate. In Ref. 15 the authors have simulated the aggregation of long flexible chains with one sticker site located at each end of the chain. This particular localization of the functional group is relevant to the study of telechelic ionomers. Reference 16 reports the aggregation process for chains with a single sticker located at one end of the chain. In that case, and for sufficient long chains, the authors obtained structures similar to reverse micelles with very few chains belonging to the aggregate which is a typical characteristic of reverse micelles as seen in experi-

 0021-9606/91/075115-11$03.00  

ments.[8] On the other hand, we have developed an alternative model,[19] based on an extension of Eden dynamics,[20] originally used for single particle aggregation. Its basic characteristic is that the new chain is added to the growing aggregate, by starting a self-avoiding random walk, from an empty nearest-neighbor site of one of the stickers belonging to the aggregate, picked at random. This method is computationally very effective in producing the clusters and, more importantly, it shares several universal features with the DLA model such as the morphology of the clusters formed are quite similar for systems composed of chains with a small fixed number of sticker sites. This can be understood by the following argument: as the length of the chain increases, the relative number of sticker sites decreases and then the sites that allow association, forming the so-called active zone, are mostly located at the surface of the cluster because of the screening effect due to the excluded-volume interactions. So, in the DLA model when a long chain reaches the cluster surface, it still spends a considerable amount of time in locating the active sites and thus the efficiency of the method in producing reasonably large size clusters becomes very low. One avoids this in the Eden type method by starting a new chain from an empty nearest neighbor site of one of the stickers in the aggregate and instantly the new chain becomes a part of the aggregate. Since in the presence of excluded volume interactions it is extremely difficult to find enough empty sites inside the cluster to be able to put a chain there, the active zone almost always remains at the surface of the aggregate in the Eden method as well. Thus, unlike the single particle aggregation case, here these two methods share universal features such that the exponents characterizing the radius of gyration of the aggregates are similar.[18]

Since our previous work on the Eden type dynamics has been restricted to two dimensional systems, its application to real three dimensional system is somewhat limited. One expects that the dimensionality of the aggregate would play an essential role in determining its characteristics. In this paper we have extended the Eden dynamics method in order to study the more experimentally relevant case of the clustering process in a three dimensional model. The structures generated via this method allow us to visualize the growth and changes in the aggregate. We can then examine how variations of polymer properties, such as the chain length, alter the clustering process. We have studied the functional dependence of the radius of gyration $R_g$, with the chain length $n$, and the number of chains $N$, in the growing cluster. We have found that the radius of gyration verifies a scaling relation of the form $R_g \approx n^{\alpha} N^{\beta}$. The calculated values of the exponents $\alpha$ and $\beta$ are lower than those predicted by an extension of Flory's classical theory. This is similar to what happens in two dimensions. It has been argued[15] that the presence of self loops causes the cluster to contract in size, resulting in a small deviation from the predicted exponent relating $R_g$ and $N$. We believe, however, that the reason for $\beta$ to be less than the theoretical value is that the sizes of the clusters studied in the simulation are not large enough to enter the asymptotic scaling regime. To support this explanation, we have obtained an exact lower bound for the exponent $\beta$ which takes into account the finite size of the chain length $n$ in the simulation. We have also considered the contribution of the three body interactions, absent in the Flory's theory and its influence over the value of the exponent $\alpha$. This contribution partially explains the values obtained for this exponent in the simulation. In contrast to the situation in two dimensions,[16,19] we haven't been able to find "frozen" structures (unable to grow any further) for chains with only one sticker site that characterize reverse micelles for sufficient long chains as observed in experiments. Our simulations can continue for a long time, though each time it is more difficult to add new chains to the cluster. However, we note that for these long times in which the rate of growing of the aggregate is very slow, other effects not considered here would be relevant in the growing process in experimental situations. These include the presence of interaction effects between different micelles and fragmentation processes.

The rest of the paper is organized as follows: In Sec. II we describe the numerical model. In Sec. III we present the results for the aggregation of telechelic ionomers. In Sec. III A we carry out a Flory type mean field calculation of the exponents $\alpha$ and $\beta$ and consider the effect of three body interactions on the exponent $\alpha$. In Sec. III B we obtain a geometric lower bound for the exponent $\beta$. In Sec. IV we present the corresponding results for reverse micelles. Section V concludes with a discussion of the results and possible extensions of our work.

## II. NUMERICAL MODEL

The model used in our simulations is an extension of the Eden type dynamics developed in Ref. 19. A polymer of degree of polymetrization $n$ is modeled by a self-avoiding random walk of $n-1$ bonds in a simple cubic three dimensional lattice with $L \times L \times L$ sites. For telechelic ionomers two sticker sites are located one at each end of the chain. Reverse micelles, on the other hand, will be formed by chains containing just one sticker site in one of the ends. All the chains in the simulation obey the excluded volume criterion, so that no lattice site can be occupied by more than one monomer at a time. No other interactions are considered between chains. For ionomers, the growing process starts by placing a seed chain with one of its two stickers located at the center of the lattice. After placing the first chain an integer random number between 1 and $n$ is generated. If the random number is 1 we will try to add a new chain, given by a self-avoiding random walk, starting at a randomly chosen empty nearest-neighbor site of one of the sticker sites (chosen at random). If the random number equals $n$, the $n$th monomer, a sticker site, if not already stuck to another polymer, is tried to move to a randomly chosen empty nearest-neighbor site of the $n-1$th monomer. Finally, if a nonsticking bead located at $r_i$ is chosen, corresponding to a random number between 2 and $n-1$, the chain dynamics is simulated by the following process: First the bead at location $r_i$ is tried to move by using the Verdier–Stockmayer algorithm.[21] The new position $r_i'$ is given by

$$\mathbf{r}_i' = \mathbf{r}_{i+1} + \mathbf{r}_{i-1} - \mathbf{r}_i, \tag{1}$$

*where* $\mathbf{r}_{i+1}$ *and* $\mathbf{r}_{i-1}$ *are the locations of the* $i+1$th and $i-1$th beads, respectively. The final position $\mathbf{r}_i'$ *is accepted*

only if it is not already occupied by another bead. Otherwise, a cranckshaft motion is tried. This movement involves the monomers $i$th and the $i-1$th. The new positions are the following:

$$\mathbf{r}_j' = \mathbf{r}_j + \mathbf{v} \quad j = i, \quad i-1, \tag{2}$$

where $\mathbf{v} = \mathbf{a}_j \pm \mathbf{a}_{j-1} \times \mathbf{a}_j$ and $\mathbf{a}_j = \mathbf{r}_{j+1} - \mathbf{r}_j$ is the $j$th bond vector of the chain. The two signs that appear in $\mathbf{v}$ (chosen again randomly) indicate the clockwise or counterclockwise sense of the rotation.

When there is more than one chain present in the cluster, we first randomly chose a chain and then chose a random bead from this already selected chain and proceed on the way described above. The aggregation process continues until there are a prescribed number of chains present in the cluster.

The model and the numerical procedure for the aggregation process for reverse micelles are similar to the above case, except that the chains have just one sticker site located at one of the ends of the chain.

## III. AGGREGATION OF TELECHELIC IONOMERS

In order to investigate the influence of the chain length and the number of chains in the morphology of the aggregate, we have carried out extensive computer simulations varying the chain length from $n = 2$ to $n = 50$ and the number of chains from $N = 10$ to $N = 7500$.

Figures 1 and 2 show characteristic morphologies of the aggregates for $n = 10$ and $n = 50$, respectively. We notice in both cases the presence of a gel type extended network, which can in principle fill out as large a volume as one desires. This is truly independent of the chain length. The aggregates are diffuse and basically irregular in shape.

These kind of structures generated by irreversible growth can be described by fractal exponents relating the number of particles of the aggregate with a characteristic linear size, such as the radius of gyration. In order to investigate the possible fractal nature of the telechelic ionomer aggregates generated in our simulation, we are interested in a scaling law relating the radius of gyration $R_g$ with the number of chains $N$, and the chain length $n$. As discussed in Refs. 15, 16, and 19 the mass $Nn$ is inappropriate as a single variable, since the entropy plays an important role in deciding the linear size and the shape of the aggregates. So, one postulates that $R_g$ depends on $n$ and $N$ separately, i.e.,

$$R_g \approx n^{\alpha} N^{\beta}. \tag{3}$$

The exponents $\alpha$ and $\beta$ characterize the size of the aggregate and are expected to depend on the dimensionality. In order to calculate the exponent $\alpha$ we have computed the radius of gyration for $N = 50, 100, 200, 500, 1000$ chain clusters for different values of the chain length, ranging from $n = 2$ to $n = 50$. After averaging over 100 configurations, we plot in Fig. 3 the logarithm of the radius of gyration $R_g$ vs the logarithm of the chain length $n$. The straight lines in this figure are the best fit to the data. The computed values for $\alpha$ for these different $N$ values can be well described by $0.45 \pm 0.05$ although there is some systematic downward trend in the value of $\alpha$ as $N$ increases. The exponent $\beta$ is calculated in a similar way. Fixing $n$, we find the radius of gyration when the number of chains belonging to the aggregate varies from $N = 10$ to $N = 7500$, for $n = 2,5$; from $N = 10$ to 2500 for $n = 10$ and from $N = 10$ to 1000 for $n = 25$. From the best fits to the points on Fig. 4 we obtain that the values for $\beta$ for these different $n$ values can be well described by $0.27 \pm 0.05$. Here also we note a downward trend in $\beta$ as $n$ increases indicating that the clusters of these sizes are yet to enter the true scaling regime. To stress the relationship (3), we have plotted $\log(R_g/n^{\alpha})$ vs $\log(N)$ taking $\alpha = 0.45$ (Fig. 5). We observe that all the data collapse reasonably well in a single master curve; we also include in this figure a solid line of slope 0.27 to guide the eye and a dashed line with slope $\frac{1}{3}$ corresponding to the value of $\beta$ calculated from the Flory mean field theory. Thus, Eq. (3) can correctly describe the data, but the exponents $\alpha$ and $\beta$ must

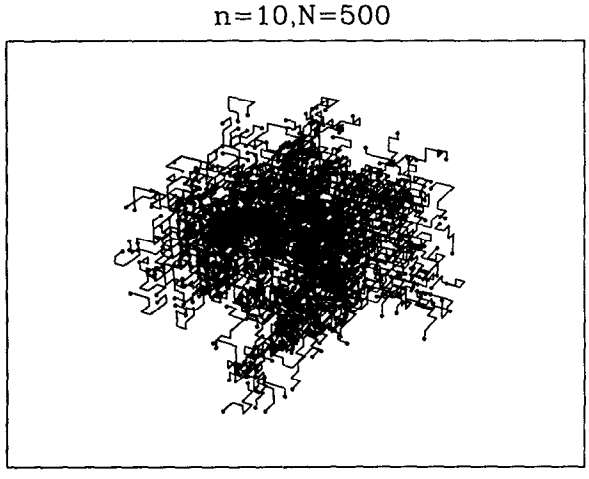


FIG. 1. Typical morphology of the aggregates for telechelic ionomers for chain length, $n = 10$ and number of chains $N = 500$. A polymer chain is represented by a series of connected sites on a simple cubic lattice. The sticker sites are represented by dots.

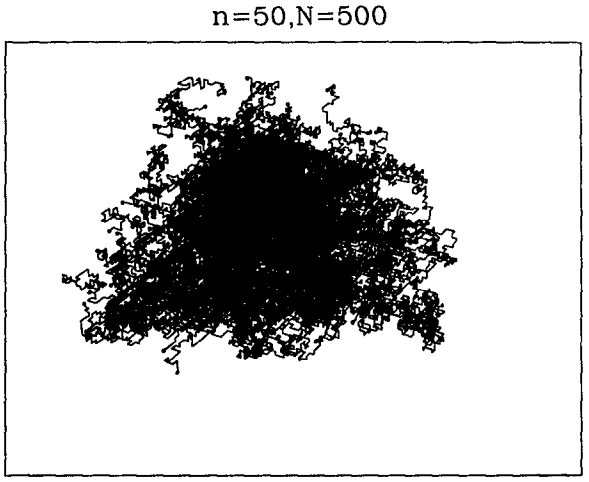


FIG. 2. Same as Fig. 1 for $n = 50$ and $N = 500$, respectively.

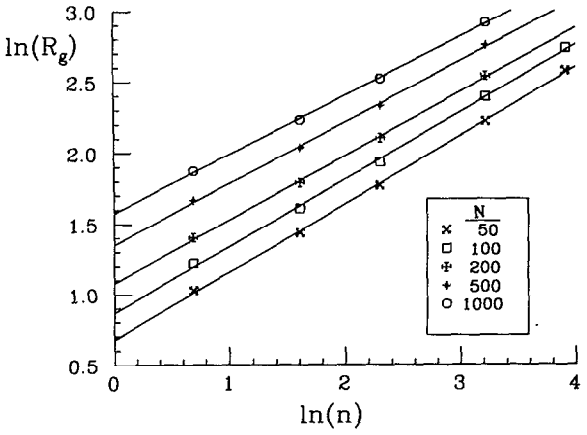


FIG. 3. Logarithmic plot of the radius of gyration $R_g$ vs the number of beads $n$ for several values of $N$. The straight lines are the best fit to data. The exponent $\alpha$ calculated from above fits are given by $\alpha = 0.45 \pm 0.05$.

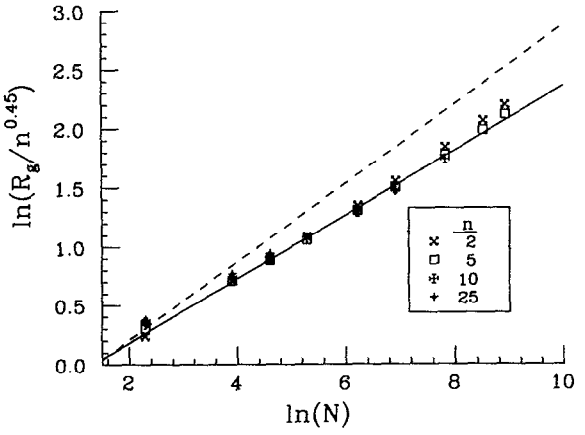


FIG. 5. Logarithmic plot of $R_g$ scaled by $n^{0.45}$ vs the number of chains $N$, for $n = 2$, 5, 10, 25, for telechelic ionomers. The maximum number of chains for each aggregate is: $N = 1000$ for $n = 25$, $N = 2500$ for $n = 10$, and $N = 7500$ for $n = 2,5$. The straight line of slope 0.27 is a guide to the eye and the dashed line has a slope equal to the theoretical value $\beta = 1/3$.

be considered as effective exponents as we will discuss shortly.

We have also computed the probability density function for the radius of gyration $P(R_g)$ for different values of $n$ and $N$ by taking averages over 100 configurations $g$ in each case. We have found that $P(R_g)$ can be approximated reasonably well by a phenomenological fit to a Gaussian distribution, as shown in Fig. 6.

In the next section we discuss the classical Flory theory in the context of network formation from monodisperse polymer chains in three dimensions, and calculate the exponents $\alpha$ and $\beta$ within the framework of this theory. We then go on to discuss the effect of the finite size of the samples and the presence of higher order interaction terms on the values of $\alpha$ and $\beta$ as computed in the numerical simulations.

### A. Flory's mean field approximation

In order to compute the free energy associated with one of the aggregates, we will start by considering the simplest realization of a polymer chain: Orr's (Gaussian or ideal) chain model in which a polymer is represented by an unrestricted random walk on a periodic lattice. The free energy of such a chain as a function of the end-to-end distance $r$ is given by[22]

$$F_n(r) = F_n(0) + \frac{dT}{2n} r^2 - (d-1)T \log(r), \qquad (4)$$

where $d$ is the space dimensionality, $T$ the absolute temperature, and $n$ the chain length (the lattice spacing has been taken equal to 1).

When considering a self-avoiding chain we must include in the previous expression the $z$-body interaction term originated by the application of the excluded volume criterion. This term causes the radius of gyration of the chain to be greater than that of a Gaussian chain. Below a critical dimension, then, the chain with the same mass has a linear

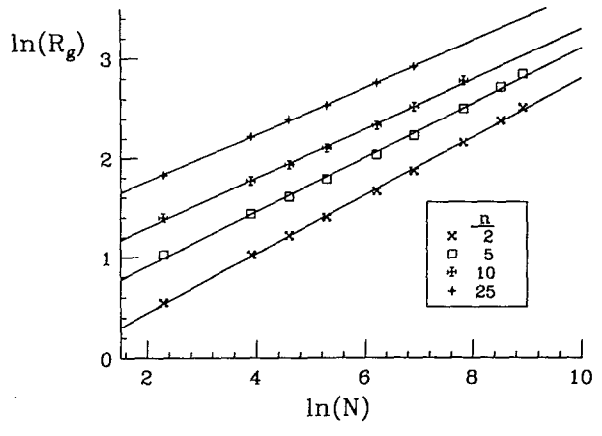


FIG. 4. Logarithmic plot of $R_g$ vs $N$, for different values of the chain length $n$. The straight lines are the best fit to the data. The exponent $\beta$ calculated from above fits are given by $\beta = 0.27 \pm 0.05$.

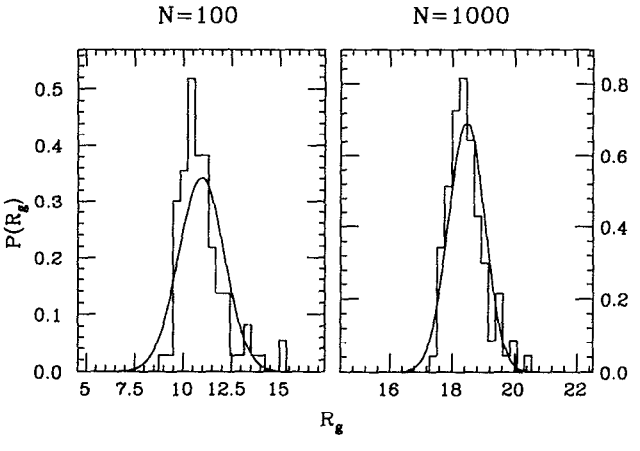


FIG. 6. Probability density function $P(R_g)$ for the radius of gyration for $n = 25$ and $N = 100$ and 1000. The histograms obtained are fitted by a phenomenological Gaussian distribution.

extension larger than the ideal chain; we look for a functional dependence for the mean end-to-end distance $\langle r\rangle = r_0 \approx n^{\nu}$ with $\nu > \frac{1}{2}$ (where the symbol $\approx$ stands for the asymptotic leading behavior for large $n$).

The $z$-body interaction term can be written as $\omega T C^z r^d/2$, where for $z=2$, $\omega = (1-2\chi)$ is the excluded volume parameter and $\chi$ the Flory's interaction parameter; $\chi = 0$ for ideal solvents and $\chi < \frac{1}{2}$ for good ones. $C$ is the local concentration of monomers, $C = n/r^d$. The interaction term becomes

$$\frac{\omega T}{2} n^z r^{-(z-1)d}. \tag{5}$$

Adding this term to (4) and minimizing the resulting expression with respect to $r$, we get

$$\frac{dr_0}{n} = \frac{d-1}{r_0} + \frac{\omega(z-1)}{2} n^z r_0^{-(z-1)d-1}. \tag{6}$$

Assuming $r_0 \approx n^{\nu}$ and considering the $n$ dependence only we get

$$n^{\nu-1} \approx n^{-\nu} + n^{z-(z-1)d\nu-\nu}. \tag{7}$$

If we assume $-\nu < z-(z-1)\,d\nu-\nu$ or equivalently $\nu < z/[(z-1)d]$, then the first term of the rhs of Eq. (7) is negligible compared to the second one for large $n$. Equating the powers of the leading term in $n$ of both sides we get

$$\nu - 1 = z - (z-1)d\nu - \nu$$

or

$$\nu = \frac{z+1}{2+(z-1)d} \tag{8}$$

valid for $d < (2z/z-1) = d_c$. Whereas for $d \geqslant d_c$ (the critical dimension) we have $\nu = \frac{1}{2}$.

For $d=3$ and considering only two-body interactions ($z=2$), we recover the results of Flory's theory $\nu = \frac{3}{5}$. If only three-body interactions are allowed ($z=3$) then $\nu = \frac{1}{2}$, lower than the previous one.

We now assume that the mean end to end distance $r_0$, is proportional to the radius of gyration of a single chain, $R_0$. Furthermore, we consider that every chain is a fully equilibrated self-avoiding random walk at every stage of the aggregate growth, thus, the aggregate is expected[15] to have a size such that its monomer concentration, $Nn/R_g^d$, is proportional to the monomer concentration of a chain, $n/R_0^d$ (the so called overlap threshold concentration $C^*$):

$$C^* = n/R_0^d \propto Nn/R_g^d. \tag{9}$$

Assuming $z=2$, $R_0 \approx n^{3/(d+2)}$ so that the radius of gyration scales as

$$R_g \approx N^{1/d} n^{3/(d+2)}. \tag{10}$$

The values predicted for the exponents by this relation are, assuming $d=3$, $\alpha = \nu = \frac{3}{5}$ and $\beta = \frac{1}{3}$ ($\beta = 1/d$ in general dimensions). However, the values for the exponents obtained from the numerical simulation are lower than those predicted by Eq. (10). The same discrepancy was seen in the previous two-dimensional studies.[15,19]

In order to explain the fact that the value for $\alpha$ in the simulation is smaller than the value obtained on Flory's theory, let us consider the effect of the three-body interaction term on the radius of gyration.

We can write the free energy as:

$$F = F1 + F2 + F3. \tag{11}$$

Where $F1$, $F2$, and $F3$ represent the elastic term, the two-body interaction term, and the three-body interaction term, respectively.

For a single chain at the overlap concentration

$$\begin{aligned} F1 &\approx R_0^2/n, \\ F2 &\approx R_0^d C^{*2} \approx R_0^d (n/R_0^d)^2 = R_0^{-d} n^2, \\ F3 &\approx R_0^d C^{*3} \approx R_0^d (n/R_0^d)^3 = R_0^{-2d} n^3. \end{aligned} \tag{12}$$

For a system with $N$ chains the elastic energy term will be $N$ times the elastic energy of a single chain. For $F2$ and $F3$ we can take the same expression as before but with the monomer concentration of the cluster at the overlap threshold, $Nn/R_g^d$, so the asymptotic behavior of each term is

$$F1 \approx NR_0^2/n, \tag{13a}$$

$$F2 \approx R_g^d C^{*2} = R_g^{-d} n^2 N^2, \tag{13b}$$

$$F3 \approx R_g^d C^{*3} = R_g^{-2d} n^3 N^3, \tag{13c}$$

where $R_0$ is the radius of gyration of a single chain and $R_g$ the radius of gyration of the aggregate. They scale as $R_0 \approx n^{\nu}$, $R_g \approx n^{\alpha} N^{\beta}$. We have seen before that including the two-body interaction term [making $z=2$ in Eq. (5)], in the expression of the free energy, Eq. (4), we get $\alpha = \frac{3}{5}$; whereas, considering $z=3$, allowing three-body interactions only, the effect is to lower the value of $\alpha$ to $\alpha = \nu = \frac{1}{2}$. We are interested, then, in finding out what is the importance of $F3$ when $F2$ is also present. The asymptotic behavior of $F1 + F2$ is given by

$$\begin{aligned} F1 + F2 &\approx NR_s^2/n + R_g^{-d}(Nn)^2 \\ &\approx Nn^{2\nu-1} + N^{2-\beta d} n^{2-\alpha d}. \end{aligned} \tag{14}$$

By minimizing $F1 + F2$ with respect to $n$ we finally get $\beta = 1/d$ and $\alpha = (3-2\nu)/d$ and then

$$\begin{aligned} F1 &\approx F2 \approx Nn^{2\nu-1}, \\ F3 &\approx Nn^{4\nu-3}. \end{aligned} \tag{15}$$

If $\nu < 1$ ($d > 1$) $F3$ is less important than $F2$ but one can conclude that the effect of $F3$ is to reduce the effective value for the exponent $\alpha$ making it lower than $\nu$.

As discussed above, the presence of three-body or higher order interactions then can decrease the value of $\alpha$ from that predicted in Flory's classical theory. However, we believe that the finite size of the clusters also affect the exponents, in the sense that the clusters of these sizes are yet to enter the true asymptotic scaling regime. This is particularly true for the exponent $\beta$ as we will discuss in the next section. It was pointed out in Ref. 15 that the presence of self loops which cause the cluster to collapse could somewhat reduce the value of $\beta$. It should be noted however that such self loops are extremely rare in our simulation. We believe, then, that the numerical result $\beta < 1/d$ is due simply to the fact that the values of $N$ considered on the simulation are not large enough to enter the scaling regime in which (3) is supposed to hold fully. To support this explanation, we have obtained exact (lower) bounds of a geometrical origin for

the exponent $\beta$. These bounds turn out to reproduce accurately the values for $\beta$ obtained in the numerical study.

### B. A geometrical restriction

The radius of gyration $R_g$ of any structure formed by $N$ chains of length $n$ satisfies the geometrical restriction

$$R_g^2 = \frac{\sum_{i=1}^{Nn} r_i^2}{Nn} \geqslant R_h^2, \tag{16}$$

where $r_i$ characterizes the position of the $i$th monomer from the center of mass and $R_h$ is the radius of gyration of an hypersphere (the most compact structure possible) of mass (volume) $M = Nn$. If $R$ is the radius of the hypersphere we note $R = (\frac{5}{2})^{1/2} R_h$, for $d = 3$ and

$$M = \frac{4}{3}\pi R^3 = 4/3\pi(5/2)^{3/2} R_h^3 = C_d R_h^d,$$

where $C_d$ is a constant. From (16) we get

$$R_g \geqslant R_h = \left(\frac{Nn}{C_d}\right)^{1/d}. \tag{17}$$

By writing $R_g = AN^\beta$ we arrive at

$$\beta \geqslant \frac{1}{d} - \frac{\log A + 1/d \log(C_d/n)}{\log N}. \tag{18}$$

Here $\log(A)$ can be measured as the independent term coming from the fit of the data in the $\log(R_g)$ vs $\log(N)$ representation. Note that $\beta \to 1/d$ when $N \to \infty$.

In Table I we compare the lower bounds for $\beta$, calculated from Eq. (18) compared with the values obtained by the numerical simulation. We note, as mentioned before, that the lower bounds agree reasonably well with those values of $\beta$ found in the simulation. This supports the fact that the values of $N$ considered here although quite large (e.g., $N = 7500$) are not large enough to enter the asymptotic regime.

## IV. FORMATION OF REVERSE MICELLES

In this study we have investigated the influence of the chain length on the morphology of the cluster for two limits: short chains ($n \leqslant 25$) and long chains ($n \geqslant 50$).

For short chains we have systematically varied the length from $n = 2$ to $n = 25$ and the number of chains from $N = 10$ to 10 000 for $n = 2,3,4$; from $N = 10$ to $N = 2500$ for $n = 10$; from $N = 10$ to 500 for $n = 15$ and from $N = 10$ to 100 for $n = 25$. In Figs. 7 and 8 we show some of the typical

TABLE I. Lower bounds for $\beta$ calculated from Eq. (13) for telechelic ionomers are compared with the values of $\beta$ obtained from the simulation. $A$ is obtained from the fit to the expression $R_g = AN^\beta$.

| $n$ | $N$ | $\log A$ | $\beta$ | $\beta$(simulation) |
|---|---|---|---|---|
| 2 | 7500 | −0.14 | 0.27 | 0.29 |
| 5 | 7500 | 0.36 | 0.25 | 0.27 |
| 10 | 2500 | 0.80 | 0.22 | 0.25 |
| 25 | 1000 | 1.29 | 0.17 | 0.23 |

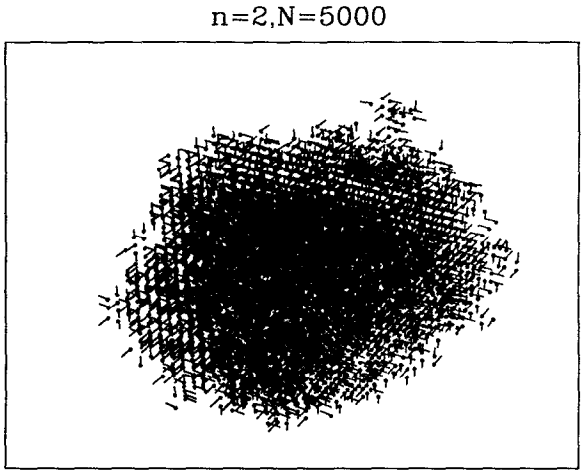


FIG. 7. Typical morphology of reverse micelles for short chains ($n = 2$) with one sticker site. The number of chains is $N = 5000$.

morphologies of those aggregates. We note that the structures formed are more compact than the ones observed in telechelic ionomers. They appear to be ellipsoidal in two dimensional cross sections as can be easily seen in Fig. 9, where we present several cross sections of the aggregate for different planes. Here we have also calculated, as in the case of telechelic ionomers, the exponents $\alpha$ and $\beta$ characterizing the asymptotic behavior of the radius of gyration as $R_g \approx n^\alpha N^\beta$. After averaging over 100 runs, we present in Fig. 10 a log–log plot of the radius of gyration $R_g$ vs the chain length $n$, for different values of $N$. From the best least squares fit to the data we obtain values for $\alpha$ as $0.45 \pm 0.05$. In order to compute the exponent $\beta$ we now fix $n$ to a particular value and represent $\log(R_g)$ vs $\log(N)$ (Fig. 11). The fit to the data gives values for $\beta$ as $0.31 \pm 0.02$. In Fig. 12 we have plotted $\log(R_g/n^\alpha)$ vs $\log(N)$, taking $\alpha = 0.45$. We also include in this figure a solid line of slope 0.31 i.e., to guide the eye and a dashed line with slope $\frac{1}{3}$, expected from Flory theory. Obviously, the bounds found on the previous section, being of a purely geometrical origin, also apply in

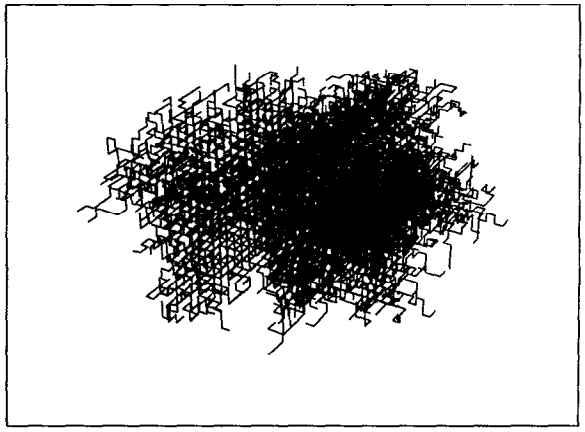

FIG. 8. Same as Fig. 7 for $n = 10$ and $N = 1000$.

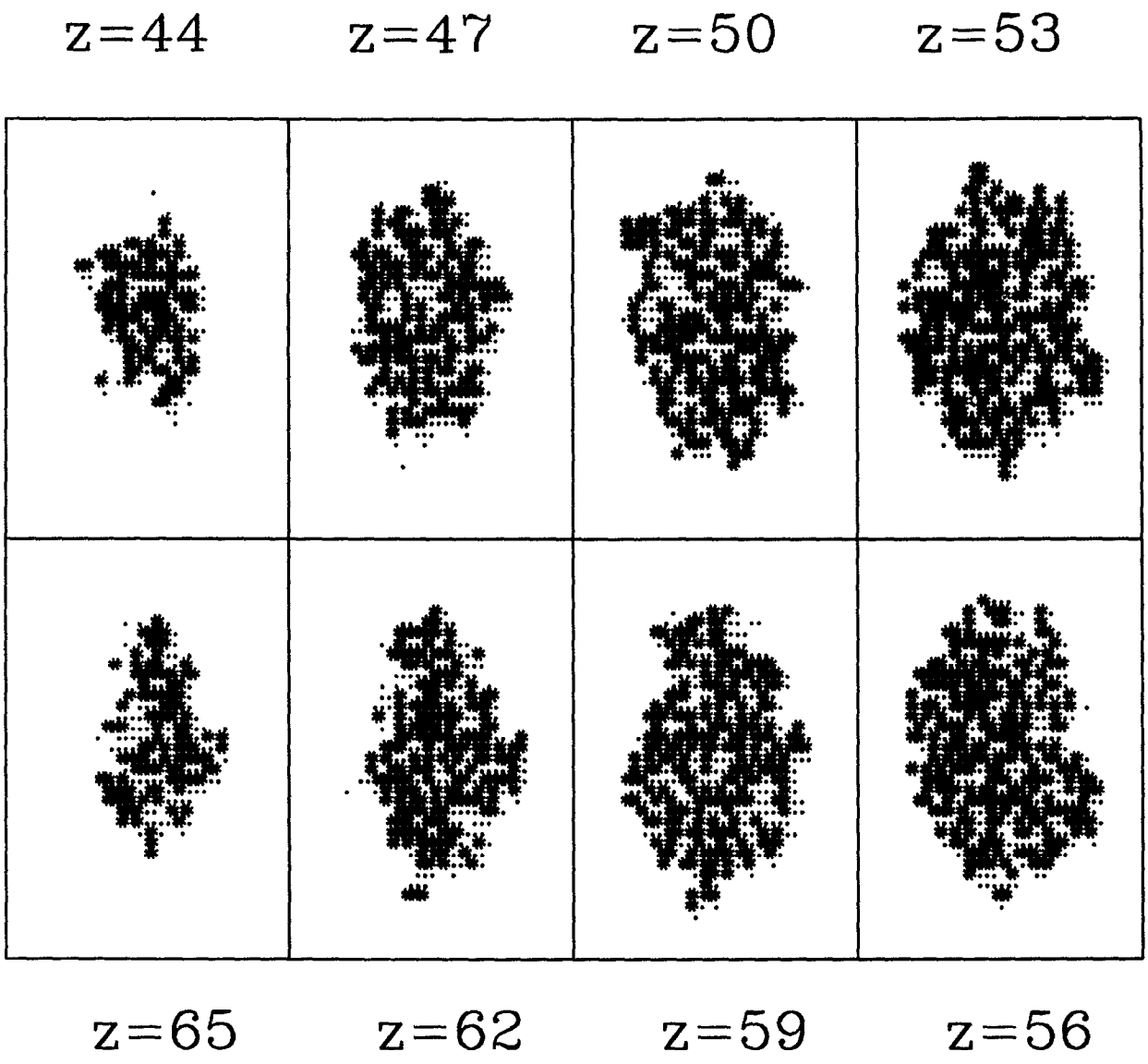


FIG. 9. Different cross sections with a vertical coordinate $z$ for a reverse micelle corresponding to $n = 2$, $N = 5000$. The middle plane is $z = 56$. These ellipsoidal shapes are a typical characteristic of these structures, as seen in experiments (Ref. 8).

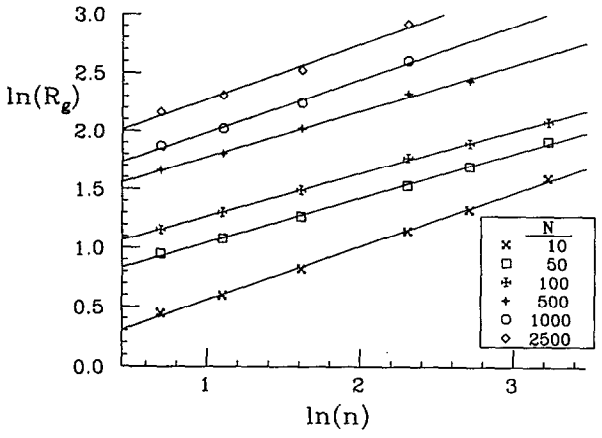


FIG. 10. Logarithmic plot of the radius of gyration $R_g$ vs the chain length $n$ for several values of $N$, for reverse micelles. The straight lines are the best to the data yielding $\alpha = 0.45 \pm 0.05$.

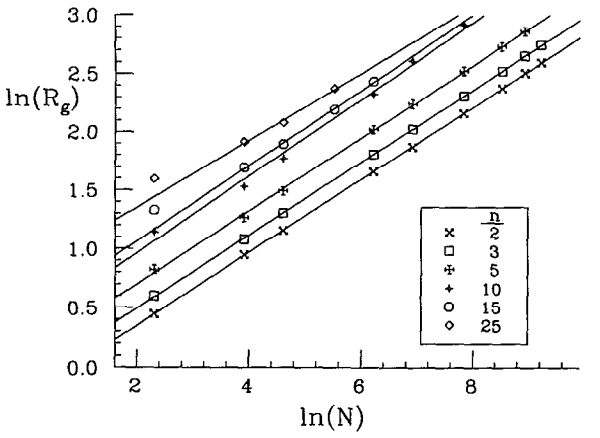


FIG. 11. Logarithmic plot of $R_g$ vs $N$, for different values of the chain length $n$ for reverse micelles. The straight lines are the best fit to the data yielding $\beta = 0.31 \pm 0.02$.

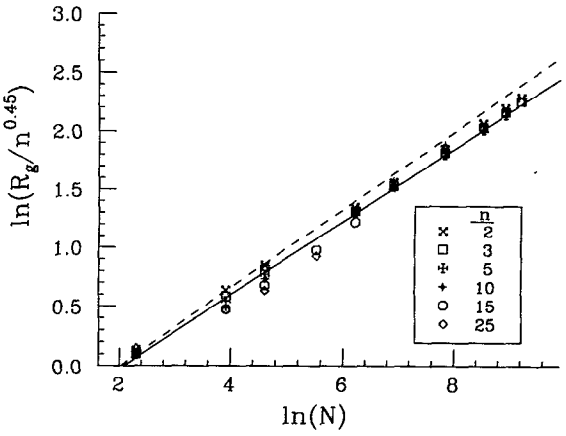


FIG. 12. Logarithmic plot for reverse micelles of $R_g$ scaled by $n^{0.45}$ vs the number of chains $N$ for $n = 2, 3, 5, 10, 15, 25$. Note that most of the data obtained collapse on a single master curve. The maximum number of chains for each aggregate is: $N = 1000$ for $n = 2,3$; $N = 7500$ for $n = 5$; $N = 2500$ for $n = 10$; $N = 500$ for $n = 15$; $N = 100$ for $n = 25$. To guide the eye we include a straight line of slope 0.31. The dashed line corresponds to the theoretical value $\beta = \frac{1}{3}$.

this case. We show in Table II the values obtained for $\beta$ in our simulations for each $n$, and the corresponding bound values calculated from Eq. (13) where we have considered the highest value for $N$. Note that as $N$ increases, the bound values agree better with those found in our simulations.

We now turn to the study of long chains. Figure 13 is an example of these structures. They seem irregular in shape and they are less compact than the clusters generated with short chains. We also represent in Fig. 14 several cross sections. Figure 15 shows the radial density as a function of $r$, for different values $n$ and $N$. For small $n$ ($n < 10$) we can see a plateau corresponding to a compact and homogeneous

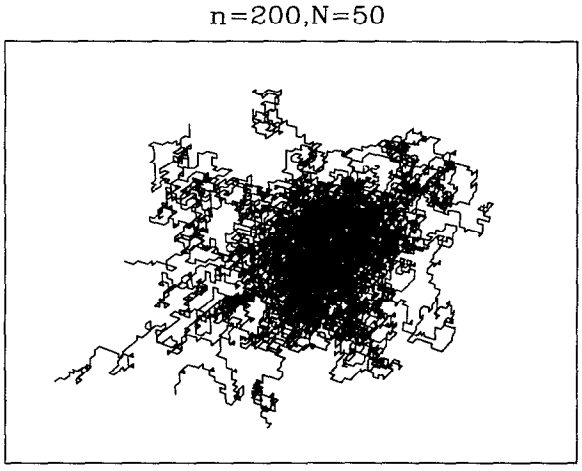


FIG. 13. Morphology obtained for reverse micelles with long chains ($n = 200$) for $N = 50$.

TABLE II. Same as in Table I for the case of reverse micelles.

| $n$ | $N$ | log ($A$) | $\beta$ | $\beta$(simulation) |
|---|---|---|---|---|
| 2 | 100 00 | −0.27 | 0.28 | 0.31 |
| 3 | 100 00 | −0.13 | 0.28 | 0.31 |
| 5 | 750 0 | 0.07 | 0.28 | 0.31 |
| 10 | 250 0 | 0.30 | 0.27 | 0.33 |
| 15 | 500 | 0.42 | 0.26 | 0.32 |
| 25 | 250 | 0.78 | 0.22 | 0.28 |

core for $r \ll R_g$, then the density drops quickly to zero. For longer chains the density appears as a rather smooth curve due to the inhomogeneities and less compact form of the clusters.

In two dimensional studies a critical chain length $n_c$ was found, such that for $n < n_c$ the chains form an extended network and for $n > n_c$ the tails would sterically hinder a new chain from attaching to the aggregate because of the excluded volume effect, generating "frozen" structures. This does not seem to be the case at the present three dimensional study, where we can add to the cluster as many chains as we want. However a word of caution is required. As the aggregate grows, an increasing amount of time (as measured by the number of trials) is needed to successfully add a new chain into the aggregate already formed. The rate of growth of the aggregate diminishes very much as its size increases. In real systems fragmentation processes will also be present and the aggregation will be reversible. When these processes are included the dynamics will drive the system to a steady state characterized by aggregates with a limited number of chains belonging to them, as already seen in a recent three-dimensional study.[17]

## V. CONCLUSIONS

In this paper we have studied the aggregation process for self-associating flexible polymer in three-dimensions, focusing our attention on the clustering of telechelic ionomers and the formation of reverse micelles. In order to simulate this process we have used a dynamical model based on an extension of Eden's method. This model was successfully used previously in a two-dimensional simulation. This model has been shown to share some common features in two dimensions with a diffusion limited aggregation type model. Our model, despite its simplicity, qualitatively reproduces some structures observed in experimental systems. However, contrary to the experience in two dimensions, here we have not found any "frozen" structure that characterizes reverse micelles for sufficient long chains. The long time taken to add new chains to the aggregate and the absence of interactions between reverse micelles and fragmentation processes may partially explain these differences with real experimental situations. We have calculated the radius of gyration of the cluster and related it to the chain length and the number of chains belonging to the aggregate. Deviations observed from the theoretical values for the exponents $\alpha$ and $\beta$, calculated from the Flory theory, can be explained by the fact that the sizes of the cluster studied in our simulations are

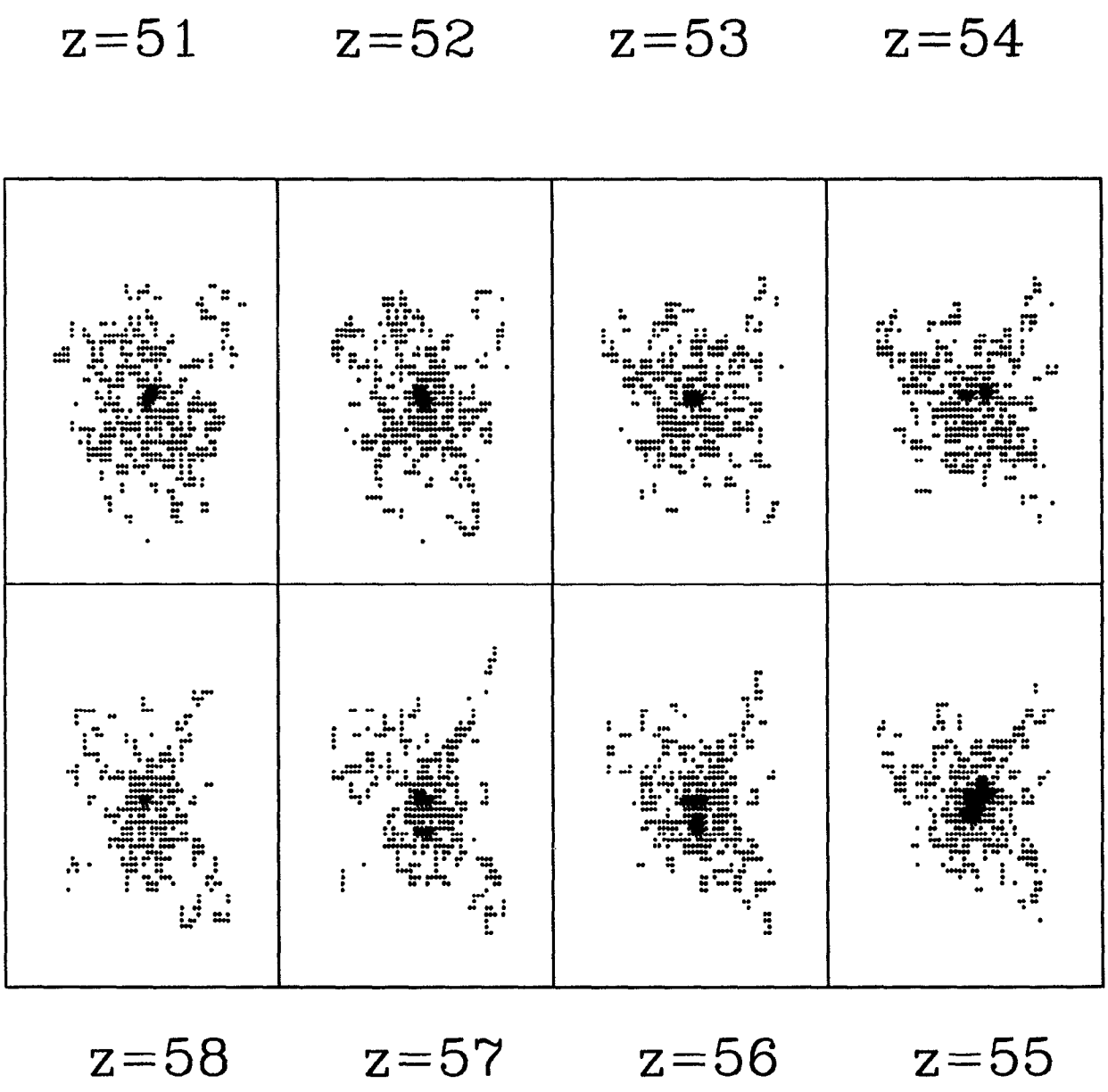


FIG. 14. Several cross sections for reverse micelles with $n = 200$, $N = 50$. We show 8 cuts through parallel planes from $z = 51$ to $z = 58$. The middle plane is $z = 55$.

not large enough to enter the asymptotic scaling regime. We have found an exact bound for $\beta$ for finite clusters and have shown that the presence of three body interactions, included as an extension of Flory's theory can cause $\alpha$ to be lower than the predicted theoretical value. We have also computed the probability density function for the radius of gyration for the telechelic ionomer model and found that it is well fitted by a Gaussian distribution. Density profile for reverse micelles are also computed and we have found that for short chains, a plateau is present characterizing compact and homogeneous structures.

Our simplified model can be improved in order to make it more realistic. We are currently extending our work to polymer systems defined without the constraint of a regular lattice. Possible modifications include the possibility of allowing fragmentation processes and also of assigning different probabilities to the sticking process depending on temperature through a Metropolis type algorithm.

## ACKNOWLEDGMENT

Financial support from the Dirección General de Investigación Científica y Tecnica (Grant No. PB-86-0534, Spain) is acknowledged.

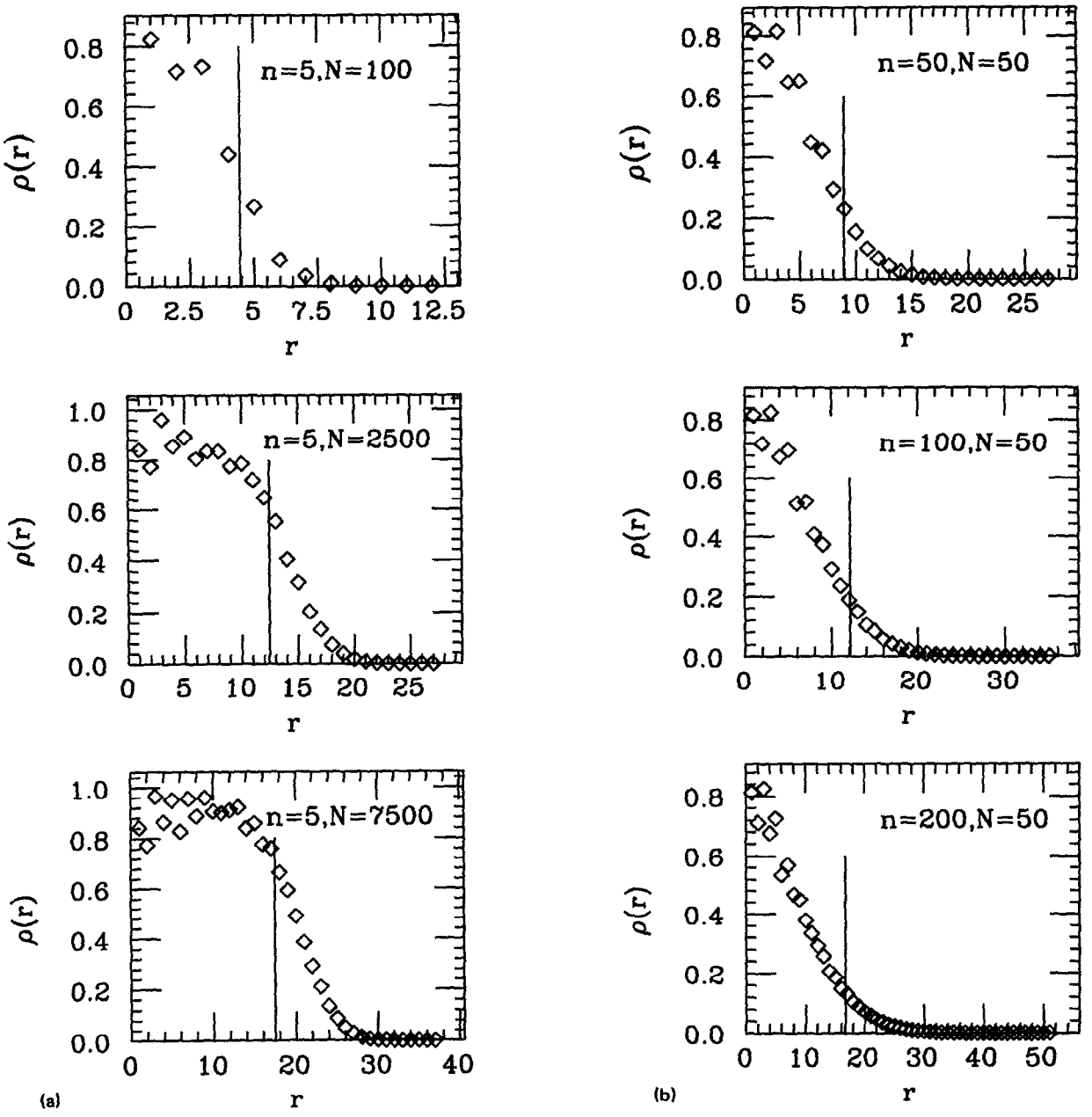


FIG. 15. (a) Radial density, $\rho(r)$, for the case of reverse micelles as a function of $r$ from the center. For $n = 5$ and $N = 100$, 2500, and 7500. The vertical lines indicate the radius of gyration associated to each cluster. We can see a plateau in density for $r < R_g$. (b) Same as before for $N = 50$ chains and chain lengths $n = 50$, 100, 200. Observe that now the radial density appears as a monotonically decreasing function of $r$ and the plateau does not appear anymore.


[1] J. N. Israelachvili, *Intermolecular and Surface Forces with Applications to Colloidal and Biological Systems* (Academic, New York, 1985).
[2] A. Eisenberg, Macromolecules **3**, 147 (1970).
[3] L. Holliday, *Ionic Polymer* (Halstead, New York, 1975).
[4] A. Eisenberg and M. King, *Ion Containing Polymers* (Academic, New York, 1977).
[5] I. Duvdevani, P. K. Agarwal, and R. D. Lundberg, Polym. Eng. Sci. **22**, 499 (1982).
[6] W. J. MacKnight and T. R. Earnest, Macromol. Rev. **16**, 41 (1981).
[7] J. H. Fendler and E. J. Fendler, *Catalysis in Micellar and Macromolecular Systems* (Academic, New York, 1975).
[8] H. F. Eicke, in *Micelles*, edited by M. J. S. Dewar (Springer, Berlin, 1980).
[9] F. Menger, Acc. Chem. Res. **12**, 111 (1979).
[10] Z. A. Schelly, in *Aggregation Process in Solution*, edited by E. Wyn-Jon and J. R. Gormally (Elsevier, Amsterdam, 1983).
[11] *Reverse Micelles, Biological and Technological Relevance of Amphiphi Structures in Apolar Media*, edited by P. L. Luisi and B. E. Straub (Pl num, New York, 1982).
[12] E. J. Goethals, *Telechelic Polymers: Synthesis and Applications* (CF Press, Boca Raton, Florida, 1989).
[13] W. Kreuder, H. Ringsdorf, and P. Tschirner, Makromol. Chem. Rap Commun. **6**, 357 (1985).
[14] D. Stauffer, A. Coniglio, and M. Adam, Adv. Polym. Sci. **44**, 103 (198
[15] A. C. Balazs, C. Anderson, and M. Muthukumar, Macromolecules 1999 (1987).

[16] A. C. Balazs, F. E. Karasz, and W. J. MacKnight, Cell Biophys. **11**, 91 (1987).
[17] A. C. Balazs, J. Y. Hu, A. P. Lentvorski, S. Lewandowski, and C. Lantman, Phys. Rev. A **41**, 2109 (1990).
[18] T. A. Witten and L. M. Sander, Phys. Rev. Lett. **47**, 1400 (1981).
[19] A. Chakrabarti and R. Toral, J. Chem. Phys. **91**, 5687 (1989).
[20] M. Eden, in *Proceedings of the Fourth Berkeley Symposium on Mathematical Statistics and Probabilities*, edited by F. Neyman (Univ. of California, Berkeley, 1961), Vol. IV. See also *Kinetics of Aggregation and Gelation*, edited by F. Family and D. Landau (North Holland, New York, 1984).
[21] P. H. Verdier and W. H. Stockmeyer, J. Chem. Phys. **36**, 227 (1962); C. Domb, Adv. Chem. Phys. **15**, 229 (1962); H. J. Hilhorst and J. M. Deutch, J. Chem. Phys. **63**, 5153 (1975).
[22] P. G. deGennes, *Scaling Concepts in Polymer Physics* (Cornell University Press, 1979).